Modeling combustion-to-detonation transition of a hydrogen-air mixture using global kinetic mechanism

Zhuchkov R.N.[1], Kozelkov A.S. [1-3], Yurlova I.A. [1], Struchkov A.V.[1,2]

) Russian Federal Nuclear Center – All-Russian Scientific Research Institute of Experimental Physics (RFNC-VNIIEF) Nizhny-Novgorod Region, Sarov.
2) Nizhny Novgorod State Technical University n.a. R.E. Alekseev, Nizhny Novgorod.
3) Moscow Aviation Institute (National Research University), Moscow, Russia

The paper presents the results of the research on the combustion-to-detonation transition of a hydrogen-air mixture basing on numerical solution of the Navier-Stokes equation system using the finite volume method on a structured mesh. It has been shown that a one-step explicit Godunov scheme results into numerical oscillations in the solution. To suppress oscillations, it is proposed to use a multi-step scheme based on the Godunov method - a Runge-Kutta type scheme. This scheme uses a hybrid modification, where there is no re-computation of diffusion flows at each internal step, while using mixing of terms from different steps, which reduces computational costs and increases the stability of the difference scheme. The combustion process is described by a global kinetic mechanism, where a single hydrogen oxidation reaction is used replacing the whole stage of the real kinetic process. We obtained the dependence of the combustion mode on molar fraction of hydrogen in the mixture.

The study was supported by the Science and Universities National Project, a part of Program of the Ministry of Education and Science of the Russian Federation to Establish Laboratories for Young Scientists, Project No FSWE-2024-0001 (Using Exa- and Zetta-Flop Supercomputers for Developing the Numerical Methods, Models and Algorithms to Describe Gas and Fluid Flows in Nature and the Industrial Facilities Functioning in Normal and Critical Conditions), as well as the program for development of the world-class scientific center “Supersonic” in 2020–2025 with the financial support of the Ministry of Science and Higher Education of the Russian Federation (Agreement dated April 20, 2022, No. 075-15-2022-309).

Introduction

Computational gas dynamics has now become a powerful tool for justifying technical characteristics of industrial products, optimizing their workflows and predicting flow parameters in different applications. The system of Navier-Stokes equations, for approximation of which on an unstructured mesh the method of finite volumes is used, is the main system of numerical solution of fundamental and industrial problems of computational fluid dynamics [1-3]. When solving problems of gas dynamics, the accuracy of determining the characteristics of compressible currents directly depends on the approximation order and the types of selected flow calculation schemes. In practice, they usually use schemes that have a clear physical interpretation and use solutions to the Riemann problem [4-5].

From the point of view of numerical modeling, one of the most complex processes of gas dynamics is chemical kinetics, which describes the interaction of a different number of reacting materials [6]. For the numerical study of chemical transformations, special methods have been developed and applied; they are called detailed, skeletal, reduced and global kinetic mechanisms. As a result, a complete mathematical model based on the system of Navier-Stokes equations, supplemented by equations of turbulence models and equations of chemical kinetics, makes it possible to describe the interaction of heat release due to chemical reactions, molecular transfer of heat and mass with turbulent pulsations [7].

The use of the detailed kinetic mechanism (DKM) is under development for a long time and is described in the works by many authors. Thus, in [8] DKM is proposed to describe the oxidation and combustion of iso-octane. The authors of [9] use DKM to

determine the concentration of carbon dioxide and oxygen during the oxidation of methane in a flow reactor. The results of the work [9] are of particular interest, as they are compared with an experiment. The influence of turbulent mixing mechanisms and chemical kinetics on hydrogen combustion in supersonic flows is considered in [10], which uses the mechanism of chemical kinetics presented by the authors of [11]. The main difficulty in using DKM to simulate combustion is that they can comprise hundreds and thousands of materials and elementary reactions [12]. In [13], 71 substances and 417 chemical reactions are considered to simulate high-temperature combustion of aviation kerosene surrogate. It should be noted that the consideration of low-temperature fuel combustion reactions in DKM leads to an increase in the number of chemicals. So, the authors of [14] considered the process of low and high-temperature combustion of a gasoline surrogate, taking into account more than 1000 substances and 4000 chemical reactions. Kinetic mechanisms of hydrocarbon oxidation are used to numerically solve the problems of combustion and detonation of acetylene-based mixtures [15]. When modeling the transition from slow combustion to detonation, the mechanism of high-temperature combustion of acetylene presented in [16] can be used within the gas dynamic computations. The main advantage of DKM is the ability to describe the real processes of molecular interactions [15] and predict all the physical features of the combustion process under the selected conditions (flame speed and temperature, ignition delay time and extinction conditions) [7].

The detailed kinetic mechanism of chemical reactions is very accurate, but often requires large computing power, which imposes restrictions in modeling real industrial products. This is because the variation of each substance is described by solving a partial differential equation. When considering a mixture of real fuels with a large number of components, a multiple increase in the computational load occurs due to the increase in the dimension of the state vector of the system, and numerical simulation of combustion becomes difficult.

It becomes necessary to reduce the number of independent variables (substances) and processes (reactions) used to describe fuel combustion under given conditions that do not lead to the decrease in the accuracy of the solution. To do this, simplification of the mechanism can be applied due to the exclusion of materials and reactions that do not exist under these conditions, which leads to the use of the skeletal mechanism [17]. If the time of formation of a chemical component is much less than the time of its diffusion and convective transfer, then the diffusion and convective term in the corresponding balance equation is not taken into account, due to its smallness with regard to chemical terms. As a result, the main equation is replaced by the balance equation between the formation of a chemical component and its consumption [7]. This approach underlies the reduced schemes [18], which are also a simplification of DKM.

In terms of the number of reactions and components used, the most "compact" is the global kinetic mechanism (GKM). The construction of such a mechanism is carried out by replacing the whole stage of the real kinetic process with gross reactions, a set of which describes the entire combustion process. A decrease in the number of elementary components leads to a respective decrease in the dimension of the system of differential

equations that describe chemical transformations. Thus, the global mechanism includes a relatively small number of components and reactions describing the integral stages of chemical transformations. When using GKM, the approximation of the reaction rate is performed by empirical expressions containing fitting parameters [15]. Ultimately, this results in a shorter chemical source computation time in the total integration time of the gas dynamics equations.

The application of the global mechanism in CFD is shown in [19]. According to [19], simpler GKMs can give satisfactory results in the distribution of only some basic parameters (for example, the concentration of substances, and the temperature). The paper [20] discusses the use of GKM together with the LES-model of turbulence when simulating high-speed hydrogen combustion. The authors obtained the results on determination of the ignition delay time consistent with the results using DKM in [21]. The [6] describes modeling the combustion using a global mechanism, where GKM is used to model multi-stage oxidation and self-ignition of hydrocarbons in reacting currents. The results obtained are compared with experimental data on self-ignition delays of individual hydrocarbons and reference fuels. The description of the methane combustion process is discussed in [22], where the global kinetic mechanism is used for this, and the EDC model is used to take into account turbulence. As a result, the authors showed good agreement with the experimental data on temperature characteristics, however, there is a difference in the concentration of reaction products, which indicates the need for modification of GKM.

There are papers where GKM is used to describe the combustion process when justifying the safety of nuclear power plants [23], and often the computation is carried out on structured meshes. The modern approach to solving design problems involves the use of mainly unstructured meshes [3], and that requires adaptation of computational algorithms in terms of finite-volume discretization of the system of basic equations (for example, a method for calculating the gradient of a gas-dynamic quantity when interpolating it onto the cell face [24] or determining the value of the limiter [25]). In order to speed up the computation, implicit difference schemes are used that allow computing with the Courant number value greater than one. At the same time, when solving gas dynamics problems, one of the basic computation schemes remains the explicit difference scheme underlying the shock-capturing method or the Godunov method [4-5; 26]. The choice in favor of the latter is common when computing hyper- and supersonic aerodynamics tasks, as well as when modeling fast-going macro-processes (such as combustion and explosive processes).

This work discusses the problem of combustion of a hydrogen-air mixture characterized by a possible transition of combustion to detonation [27]. The solution of the system of gas-dynamic equations is based on the use of the Godunov method - an explicit difference scheme and the computation of flows based on the solution of the Riemann problem. It has been shown that a one-step explicit scheme leads to numerical oscillations in the solution. To suppress oscillations, it is proposed to use a multi-step scheme based on the Godunov method - a Runge-Kutta type scheme. To increase its stability and reduce computational costs, a hybrid modification of the scheme is used, when there is no

recalculation of diffusion flows at each internal step and there is mixing of dissipative terms from different steps [28]. To describe the combustion process, a global kinetic mechanism is used, where a single hydrogen oxidation reaction is considered replacing the whole stage of the real kinetic process. The selected approach reproduces one scenario of interaction of chemical components, due to which the computational cost of the entire algorithm is reduced, while it remains possible to predict the speed of flame propagation at the specified setting of the problem. This combination of computational algorithms allows simulating complex chemical processes, while it can be characterized by computational economy and a stable numerical solution.

Basic equations and discretization ways

To simulate the flow of a reacting multi-material gas, a system of Navier-Stokes equations averaged according to Reynolds [29-30] can be used, which in a conservative form, in Cartesian coordinates, is written as follows (averaging signs are removed):

$$\begin{cases} \dfrac{\partial \rho}{\partial t} + \nabla \cdot \left(\rho \vec{u}\right) = 0, \\ \dfrac{\partial \left(\rho \vec{u}\right)}{\partial t} + \nabla \cdot \left(\rho \vec{u}\vec{u}\right) = -\nabla p + \nabla \cdot \left(\tau_{\mu} + \tau_{t}\right), \\ \dfrac{\partial \left(\rho E\right)}{\partial t} + \nabla \cdot \left(\rho \vec{u} h\right) = \nabla \cdot \left[\vec{u}\left(\tau_{\mu} + \tau_{t}\right) - \left(\vec{q}_{\mu} + \vec{q}_{t}\right)\right], \\ \dfrac{\partial \left(\rho c_i\right)}{\partial t} + \nabla \cdot \left(\rho \vec{u} c_i\right) = -\nabla \vec{J}_i + \omega_i. \end{cases} \quad (1)$$

In the system of equations (1), the following notations are used: ρ is density; $\vec{u}$ is the flow velocity vector with *u, v, w* components; *p* is pressure; $E = C_v T + 0.5\left(u^2 + v^2 + w^2\right)$ is total gas energy per unit mass; $h = C_p T + 0.5\left(u^2 + v^2 + w^2\right)$ is total gas enthalpy; τ_{μ} and τ_t are molecular and turbulent components of the tangential stress tensor, respectively; q_{μ} and q_t are molecular and turbulent components of the heat-flux density, respectively; *T* is temperature; $C_v = \left(C_p T - R/m\right)$ is specific heat at constant volume; C_p is specific heat at constant pressure; *R* is a universal gas constant; *m* is molar mass of the gas; c_i is mass concentration of the *i*-component of the mixture; $\vec{J}_i$ is diffusion flux vector of the *i*-component; ω_i is mass rate of the *i*-component formation; $\sum_{i=1}^{N_k} c_i = 1, i = 1 \ldots N_k - 1$, N_k is the number of components in the mixture.

The values of the molecular component of the tangential stress tensor of the Newtonian medium meet the Newton's rheological law satisfying the relationship between the viscous stress tensor and the strain rate tensor, and the components of the heat flux density vector are related to the local temperature gradient by the Fourier law [29-31]:

$$\tau_{\mu} = 2\mu(T)\left(S - \frac{1}{3} I \nabla \vec{u}\right), \quad (2)$$

$$S = \frac{1}{2}\left(\nabla\vec{u} + \left[\nabla\vec{u}\right]^t\right), \tag{3}$$

$$q_\mu = \lambda(T)\nabla T, \tag{4}$$

The dynamic viscosity coefficient $\mu(T)$ and thermal conductivity coefficient $\lambda(T)$ are determined by Sutherland formula depending on the temperature of the flux [30,32]:

$$\mu = \mu_0 \left(\frac{T}{T_0}\right)^{0.5} \frac{T_0 + T_s}{T + T_s}, \tag{5}$$

$$\lambda = \lambda_0 \left(\frac{T}{T_0}\right)^{0.5} \frac{T_0 + T_s}{T + T_s}, \tag{6}$$

where μ_0 and λ_0 are dynamic viscosity and thermal conductivity coefficient, respectively, at temperature T_0, T_s is the Sutherland constant.

System of equations (1) is open due to the unknown relationship of one of the main variables of this system τ_t and q_t with averaged flow parameters. This connection can be established by additional relationships, which are generally referred to as turbulence models. Linear differential turbulence models use empirical relationships for turbulent viscosity coefficient μ_t.

In case of multi-material (or multi-component) flow computation, the diffusion flow vector of the *i*-component of the mixture are written according to Fick's law:

$$\vec{J}_i = -\rho D_{i,m} \nabla c_i, \tag{7}$$

where $D_{i,m}$ is the diffusion coefficient of the *i*-component.

To simulate the combustion process, a general record of the reaction r of the chemical interaction is used, that looks as follows:

$$\sum_{i=1}^{N_k} \nu'_{i,r} A_i \underset{k_{b,r}}{\overset{k_{f,r}}{\rightleftarrows}} \sum_{i=1}^{N_k} \nu''_{i,r} A_i, \tag{8}$$

where $\nu'_{i,r}$ is the stoichiometric coefficient of the *i*-th reactant of reaction *r*, $\nu''_{i,r}$ is the stoichiometric coefficient of the *i*-th product of reaction *r*, A_i is the *i*-th component of the mixture, $k_{f,r}$ is the velocity constant of the direct reaction, $k_{b,f}$ is the velocity constant of the reverse reaction.

An expression that defines the mass rate of formation of the *i*-component ω_i of the mixture is as follows:

$$\omega_i = \mu_i \sum_{r=1}^{N_R} \omega_{i,r},$$

$$\omega_{i,r} = \Gamma_r \left(\nu''_{i,r} - \nu'_{i,r}\right)\left(k_{f,r} \prod_{j=1}^{N} c_j^{\nu'_{i,r}} - k_{b,r} \prod_{j=1}^{N} c_j^{\nu''_{i,r}}\right), \tag{9}$$

where μ_i is molecular weight of the *i*-component , $\omega_{i,r}$ is molar rate of formation (or decomposition) of the *i*-component of the mixture in reaction *r*, N_R is the number of reactions, Γ_r is third component factor.

According to Arrhenius's law, the rate constant of a direct reaction is given by:

$$k_{f,r} = A_r T^{\beta_r} e^{-\frac{E_r}{RT}}, \tag{10}$$

where A_r is pre-exponential index, β_r is temperature index, E_r is activation energy, *R* is universal gas constant.

The velocity constant of the reverse reaction is calculated as:

$$k_{b,r} = \frac{k_{f,r}}{K_r}, \tag{11}$$

where K_r is equilibrium constant; it is determined according to the following expression:

$$K_r = exp\left(\frac{\Delta S_r^0}{R} - \frac{\Delta H_r^0}{RT}\right)\left(\frac{p_{atm}}{RT}\right)^{\sum_{i=1}^{N}\left(\nu''_{i,r} - \nu'_{i,r}\right)}, \tag{12}$$

here p_{atm} is atmospheric pressure, $\frac{\Delta S_r^0}{R}$ and $\frac{\Delta H_r^0}{R}$ are entropy and enthalpy factors, respectively:

$$\frac{\Delta S_r^0}{R} = \sum_{i=1}^{N}\left(\nu''_{i,r} - \nu'_{i,r}\right)\frac{S_i^0}{R}, \tag{13}$$

$$\frac{\Delta H_r^0}{RT} = \sum_{i=1}^{N}\left(\nu''_{i,r} - \nu'_{i,r}\right)\frac{h_i^0}{RT}. \tag{14}$$

In expressions (13)-(14) S_i^0 and h_i^0 are entropy and enthalpy of the standard state, respectively.

The above system of equations is approximated using the finite-volume method [33-34] and uses the integral formulation of the basic conservation laws. Discrete analogues of terms are recorded for control volume by summation by faces.

The finite-volume method is based on the integration of initial differential equations over the control volume. The control volumes (the mesh cells) are arbitrary polyhedrons covering the calculated domain without gaps and overlapping. Each polyhedron is limited with an arbitrary number of faces. Vertices of faces are mesh nodes. The general view of the cell is shown in Figure 1 (left).

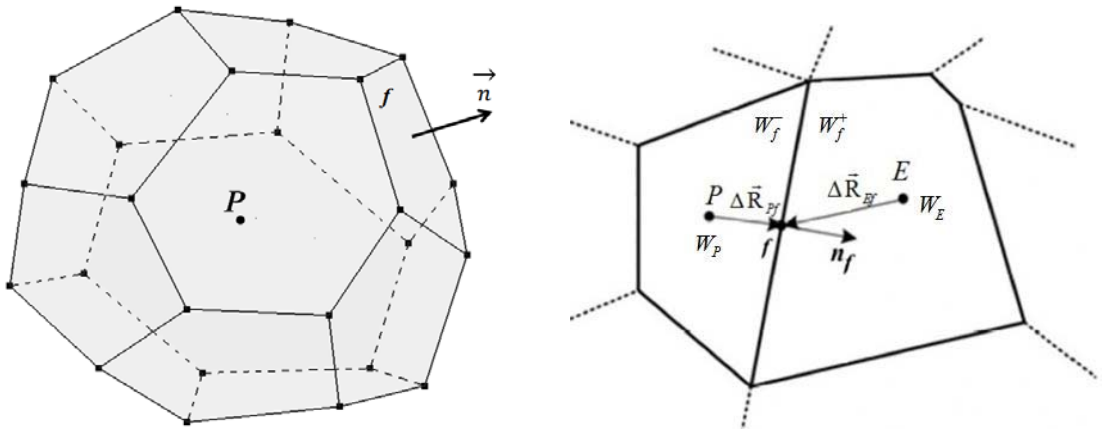

Figure 1. General view of a mesh cell (left), approximation diagram of gas-dynamic quantities (right)

We look for the solution of the initial system (1) in the area, on the boundaries of which boundary conditions of the following types can be set [35]:

- "a free boundary" - static pressure, temperature, Mach number are set;
- "an output boundary" - a fixed pressure is set, with a supersonic output flow the values are extrapolated from the boundary cell;
- "a wall" - a sticking condition, a sliding condition;
- symmetry condition;
- periodicity condition.

For a numerical solution using the finite-volume method, the Navier-Stokes equation system can be written in a vector form:

$$\frac{d}{dx}\int_{\Delta V} W dV + \oint_{\Delta\Sigma_P} (F - G) dS = \int_{\Delta V} H dV, \tag{15}$$

where vector W is a vector of conservative variables, F and G are convective and diffusion flows, H is a source term,

$$W = \begin{pmatrix} \rho \\ \rho u \\ \rho v \\ \rho w \\ \rho E \\ \rho c_i \end{pmatrix}, F = \begin{pmatrix} \rho u_n \\ \rho u u_n + p n_x \\ \rho v u_n + p n_y \\ \rho w u_n + p n_z \\ \rho H u_n + p u_n \\ \rho c_i u_n \end{pmatrix}, G = \begin{pmatrix} 0 \\ \tau_{nx} \\ \tau_{ny} \\ \tau_{nz} \\ \tau u + q \\ \rho D_{i,m} c_i \end{pmatrix} \tag{16}$$

here u_n is normal velocity component, q is heat flux, τ_{nj} is product of viscous stress tensor by normal vector.

The discrete analogue of equation (8) has the following form:

$$W_P^{n+1} = W_P^n - \frac{\tau}{V_p}\sum_{m=1}^{N_F}\left[\left[F_m - G_m\right]\Delta S\right]_f + \tau H_P^n, \tag{17}$$

where V_p is the cell volume P, τ is a time integration step, $\sum_{n=1}^{m}$ is summation by faces n of the cell P. Let's denote the total flow vector $\Pi_{P,f}$ through faces f of the cell i:

$$\Pi_{P,f} = \left[\left[F_m - G_m\right]\Delta S\right]_f . \quad (18)$$

Then expression (17) will look as follows:

$$W_P^{n+1} = W_P^n - \frac{\tau}{V_p}\sum_{m=1}^{N_F}\Pi_{Pf} + \tau H_P^n. \quad (19)$$

On the basis of an explicit difference scheme of the (19), the Godunov method was built, where convective flows are calculated by parameters on the faces determined from the solution of the Riemann problem [36].

Before you solve the Riemann problem, you should define environment parameters on the left (W_f^-) and on the right (W_f^+) from the face, i.e. to perform approximation of values. In its original form, Godunov's method assumes a piecewise-constant distribution of parameters within a cell, so "pre-breakup" parameters are considered equal to those adjacent to the cell face. This method has the first-order accuracy over space.

The Riemann problem is solved in various ways. For example, sound (or approximate) breakup dissociation or an exact solution to the self-similar breakup dissociation problem can be applied.

Eventually, for face *f* a vector of quantities on the cell face is defined (*R, U, V, W, P, E*), where *R* is density, *U, V, W* are components of the velocity vector by axes *x*, *y, z*, *P* is pressure, *E* is energy. Then the vector of convective flows for the face *f* of the cell *P* in equation (18) is determined by the formula:

$$F_f^n = F\left(W_f^-, W_f^+\right)_f^n = \begin{pmatrix} RU_n \\ RU_nU + Pn_x \\ RU_nV + Pn_y \\ RU_nW + Pn_z \\ RU_nE + PU_n \end{pmatrix}, \quad (20)$$

where U_n is normal speed, n_x, n_y, n_z are normal vector components.

To improve the order of accuracy by the spatial variable when determining parameters on the face, the Godunov-Kolgan-Rodionov scheme is used [37-39]:

$$W_f = W_P + \alpha\left(\Delta r \cdot \nabla W_P\right), \quad (21)$$

where W_P is the value of the variable in the center of the cell *P*, α is the flow restriction factor [25], Δr is the distance from the center of cell *P* to the center of face *f*, ∇W_P is the gradient value in the cell *P*.

Then the values on the left (W_f^-) and on the right (W_f^+) from the face *f* are calculated using (22) (Figure 1, on the right):

$$\begin{aligned} &W_f^- = W_P + \alpha_f^-(\Delta\vec{\mathrm{R}}_{Pf}\cdot\nabla W_P), \\ &W_f^+ = W_E + \alpha_f^+(\Delta\vec{\mathrm{R}}_{Ef}\cdot\nabla W_E), \\ &\Delta\vec{\mathrm{R}}_{Pf} = \vec{R}_f - \vec{R}_P = \left(x_f - x_P\right)\vec{i} + \left(y_f - y_P\right)\vec{j} + \left(z_f - z_P\right)\vec{k} = \Delta x_f\vec{i} + \Delta y_f\vec{j} + \Delta z_f\vec{k}; \\ &\Delta\vec{\mathrm{R}}_{Ef} = \vec{R}_f - \vec{R}_E = \left(x_f - x_E\right)\vec{i} + \left(y_f - y_E\right)\vec{j} + \left(z_f - z_E\right)\vec{k} = \Delta x_f\vec{i} + \Delta y_f\vec{j} + \Delta z_f\vec{k}; \end{aligned} \quad (22)$$

where x_i, y_i, z_i are Cartesian coordinates, $\vec{i}, \vec{j}, \vec{k}$ are unit vectors in Cartesian coordinates.

Besides, to improve the accuracy of the numerical scheme, various time conversion algorithms are used; they are called Runge-Kutta methods and underlie the creation of multi-step schemes.

Multi-step explicit hybrid scheme

In Runge-Kutta method of the m-th order of accuracy [35, 40], the solution on a new time layer is written as:

$$\begin{aligned} W_P^0 &= W_P^n, \\ W_P^1 &= W_P^0 - \alpha_1 \frac{\tau}{V_p} R_P^0, \\ W_P^2 &= W_P^0 - \alpha_2 \frac{\tau}{V_p} R_P^1, \\ &\dots \\ W_P^{n+1} &= W_P^m - \alpha_m \frac{\tau}{V_p} R_P^{m-1}, \end{aligned} \tag{23}$$

where R_P^n is a residual found by the following:

$$R_P^n = \sum_{m=1}^{N_F} \left[\left[F_m - G_m \right] \Delta S \right]_f - H_P^n. \tag{24}$$

The computational complexity of explicit multi-step schemes can be reduced if viscous flows are not recalculated at each step. In addition, dissipative terms from different steps can be mixed to increase the robustness of the difference scheme. Such methods were developed in [28] and they are known as hybrid multi-step schemes. The complexity of these methods does not exceed the complexity of conventional multi-step schemes.

Let us consider a five-step hybrid scheme, where diffusion terms are redefined in odd steps. The residual is represented as two parts:

$$\vec{R_I} = \left(\vec{R_c} \right)_I - \left(\vec{R_d} \right)_I . \tag{25}$$

The first part $\vec{R_c}$ contains central discretization of convective flows, which can be average in variables or in flows. It also contains a source term. The second part $\vec{R_d}$ consists of viscous flows numerical dissipation. For example, for central difference schemes with artificial dissipation, the discrepancies will look as follows:

$$\left(\vec{R_c} \right)_I = \sum_{k=1}^{N_F} \left[\vec{F_c} \left(\vec{W_{\alpha v}} \right) \Delta S \right]_k - \left(\vec{Q} \Omega \right)_I , \tag{26}$$

$$\left(\vec{R_d} \right)_I = \sum_{k=1}^{N_F} \left[\vec{F_v} \Delta S + \vec{D} \right]_k , \tag{27}$$

where $\vec{W_{\alpha v}}$ is the arithmetic mean of the values on the left and right sides of the face k. With the account for the residual split the scheme can be written as follows:

$$
\begin{aligned}
&\vec{W}_P^0 = \vec{W}_P^n,\\
&W_P^1 = \vec{W}_P^0 - \alpha_1 \frac{\tau}{V_p}\left[\vec{R}_c^{(0)} - \vec{R}_d^{(0)}\right]_P,\\
&W_P^2 = \vec{W}_P^0 - \alpha_2 \frac{\tau}{V_p}\left[\vec{R}_c^{(1)} - \vec{R}_d^{(0)}\right]_P,\\
&W_P^3 = \vec{W}_P^0 - \alpha_3 \frac{\tau}{V_p}\left[\vec{R}_c^{(2)} - \vec{R}_d^{(2,0)}\right]_P,\\
&W_P^4 = \vec{W}_P^0 - \alpha_4 \frac{\tau}{V_p}\left[\vec{R}_c^{(3)} - \vec{R}_d^{(2,0)}\right]_P,\\
&W_P^{n+1} = \vec{W}_P^0 - \alpha_5 \frac{\tau}{V_p}\left[\vec{R}_c^{(4)} - \vec{R}_d^{(4,2)}\right]_P,
\end{aligned}
\tag{28}
$$

where

$$
\begin{aligned}
&\vec{R}_d^{(2,0)} = \beta_3 \vec{R}_d^{(2)} + \left(1-\beta_3\right)\vec{R}_d^{(0)},\\
&\vec{R}_d^{(4,2)} = \beta_5 \vec{R}_d^{(4)} + (1-\beta_5)\vec{R}_d^{(2,0)}.
\end{aligned}
\tag{29}
$$

For central-difference and upwind difference schemes, the values of step coefficient α_m and mixing coefficient β_m are taken from Table 1.

Table 1 - Values of step coefficient α_m and mixing coefficient β_m

	Central scheme		Upwind scheme	
order	α	β	α	β
1	0.25	1	0.2742	1
2	0.1667	0	0.2067	0
3	0.375	0.56	0.502	0.56
4	0.5	0	0.5142	0
5	1	0.44	1	0.44

It is worth noting that the viscous term $\vec{R}_d$ is usually calculated only in the first two steps.

Chemical kinetics

When using models of chemical kinetics, the inclusion of source (1) directly into the Navier-Stokes equations is difficult due to the fact that the eigenvalues of the system of equations of chemical kinetics are higher than the eigenvalues of the Navier-Stokes system of equations. In this case, the component transfer equations are solved separately using the following procedure:

1. An implicit difference scheme is written as:

$$
(\rho c_i)^{n+1} = (\rho c_i)^n + \Delta t \omega_i^{n+1} \tag{30}
$$

2. Source ω_i^{n+1} is linearized by Newton:

$$\omega_i^{n+1} = \omega_i^n + \left(\frac{d\omega}{dc}\right)((\rho c_i)^{n+1} - (\rho c_i)^n) \tag{31}$$

3. The increment of the mass concentrations is found by the following formula:

$$\Delta c_i^{\gamma+1} = \left[\frac{\Theta}{\Delta t} - \left(\frac{d\omega}{dc}\right)^{\gamma}\right]^{-1} [-\frac{(\rho c_i)^{\gamma} - (\rho c_i)^n}{\Delta t} + \omega_i^{\gamma}],\ \Delta c_i^{\gamma+1} = c_i^{\gamma+1} - c_i^{\gamma} \tag{32}$$

where Δt is an integration step, Θ is the factor of safety (necessary to ensure the stability of the iterative process). Thus, expression (32) defines an iterative procedure to find the increment of mass concentrations.

The problem in solving equations (32) is to calculate the Jacobian $\left(\frac{d\omega}{dc}\right)$. Due to the fact that the user can set an arbitrary mechanism of chemical kinetics, the analytical expression of its Jacobian cannot be obtained *a priori*. This means that it must be found numerically in the process of solving a specific problem.

For clarity, let's write a formula for numerical simulation of $\left(\frac{d\omega}{dc}\right)$:

$$\left(\frac{d\omega}{dc}\right) = \begin{bmatrix} \frac{\omega_1(c_1+\varepsilon,c_2,\ldots,c_N)-\omega_1(c_1,c_2,\ldots,c_N)}{\varepsilon} & \frac{\omega_1(c_1,c_2+\varepsilon,\ldots,c_N)-\omega_1(c_1,c_2,\ldots,c_N)}{\varepsilon} & \cdots & \frac{\omega_1(c_1,c_2,\ldots,c_N+\varepsilon)-\omega_1(c_1,c_2,\ldots,c_N)}{\varepsilon} \\ \frac{\omega_2(c_1+\varepsilon,c_2,\ldots,c_N)-\omega_2(c_1,c_2,\ldots,c_N)}{\varepsilon} & \frac{\omega_2(c_1,c_2+\varepsilon,\ldots,c_N)-\omega_2(c_1,c_2,\ldots,c_N)}{\varepsilon} & \cdots & \frac{\omega_2(c_1,c_2,\ldots,c_N+\varepsilon)-\omega_2(c_1,c_2,\ldots,c_N)}{\varepsilon} \\ \vdots & \vdots & \ddots & \vdots \\ \frac{\omega_N(c_1+\varepsilon,c_2,\ldots,c_N)-\omega_N(c_1,c_2,\ldots,c_N)}{\varepsilon} & \frac{\omega_N(c_1,c_2+\varepsilon,\ldots,c_N)-\omega_N(c_1,c_2,\ldots,c_N)}{\varepsilon} & \cdots & \frac{\omega_N(c_1,c_2,\ldots,c_N)-\omega_N(c_1,c_2,\ldots,c_N+\varepsilon)}{\varepsilon} \end{bmatrix} \tag{33}$$

You see that to find the Jacobian in this way you will need to recalculate the sources of concentrations N^2 times (N is the number of concentrations). It should be noted that finding values ω_i is the most computationally loaded operation in the entire computation module, and the increase in this time by N times would have resulted into the fact that it would have taken huge computing resources to solve relatively simple problems.

To optimize the Jacobian calculation procedure, let us consider the formula that determines the rate of formation of the i-th component (for simplicity, we assume that a single reaction is defined in the system):

$$R_i = (\nu_i'' - \nu_i') k_f \prod \left(\frac{\rho c_i}{M_i}\right)^{p_{ij}}, \tag{34}$$

where ν'', ν' are stoichiometric coefficients for the i-th component, k_f is determined by formula (1.1), p_{ij} are degrees of reactants.

You see that the value $k_f \prod \left(\frac{\rho c_i}{M_i}\right)^{p_{ij}}$ does not depend on the component and can be calculated once and multiplied by the difference of stoichiometric coefficients of the *i*- th $(\nu_i'' - \nu_i')$ component in the reaction. So, to save time, in the process of calculating the first row of the Jacobian (33), a local array of size [number of concentrations] [number of reactions] is created containing values $k_f \prod \left(\frac{\rho c_i}{M_i}\right)^{p_{ij}}$ when the mass concentration of the i-

th reaction changes by a small value. This data is then used to compute the remaining rows of matrix (33).

The second assumption is that the Jacobian $\left(\frac{d\omega}{dc}\right)^{\gamma}$ does not depend on iteration γ and can be computed once on the first internal iteration of the integration of chemical kinetics equations.

The application of the above approach makes it possible to find $\left(\frac{d\omega}{dc}\right)$ matrix in time comparable to the time for calculating reaction sources ω_i, i.e. the total integration time of chemical kinetics equations increases only 2 times.

Global kinetics mechanism

Detailed reaction mechanisms give an idea of the flame structure and the reactivity of gas mixtures. However, in the case of simulating the flows in complex geometric areas, we strongly need one-step global kinetics. So, a global kinetic mechanism was proposed and substantiated, where the interaction of hydrogen and oxygen, as well as the rate of the one-stage general reaction, are determined by the modified expression proposed in [6,41]:

$$\begin{aligned} &H_2 + {}^{1}\!/\!_{2}\, O_2 = H_2O, \\ &k_{gl} = 7 * 10^{13} \exp(-{}^{20998}\!/\!_{T})[H_2]^{1.0}[O_2]^{0.5}, \end{aligned} \tag{35}$$

where k_{gl} is the reaction velocity, T is the temperature, symbols "H_2, O_2, H_2O" stand for hydrogen, oxygen and water, $[H_2]$ and $[O_2]$ are molar concentrations of unreacted hydrogen and oxygen.

This mechanism is described by the "Arrhenius" expression (10) and is used together with the described chemical kinetics to simulate the combustion of a hydrogen-air mixture.

Results of numerical simulation

We simulate the flow in a piece of pipe with ring inserts (Figure 2) [27].

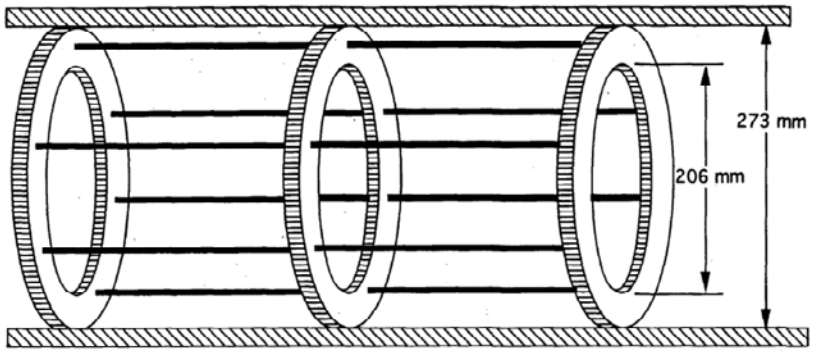

Figure 2 – Geometry of the initial model

A part of the pipe (2 m long) and a ¼ part of its circular section are considered as a computation area (Figure 3).

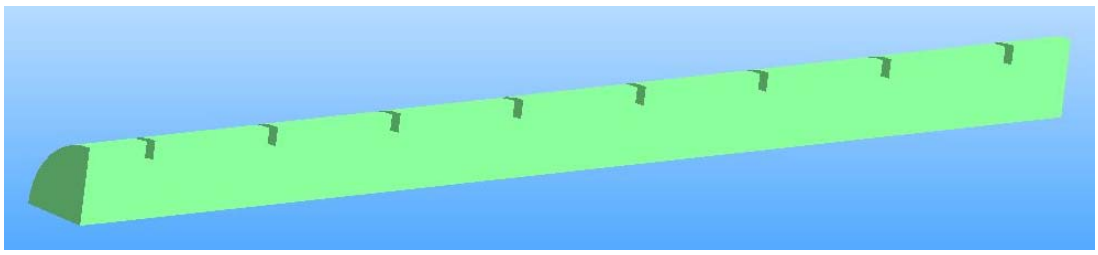

Figure 3 – Geometry of the computation area

A block-structured computation mesh (Figure 4) is used; it contains 14 million cells. Typical cell sizes are as follows: horizontally: 1e-4 m; vertically: 2e-3 m.

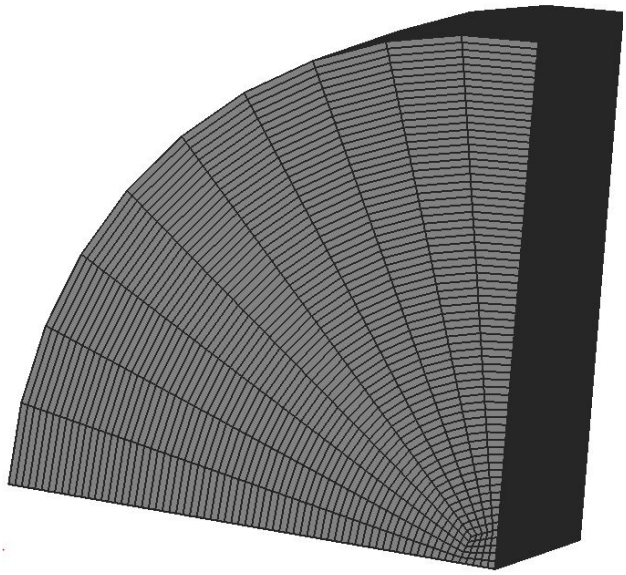

Figure 4 – A piece of the computation mesh

For integration in time, when solving the problem, a one-step explicit scheme (19) and a hybrid scheme of (28) are used. The flow is considered laminar. A second-order approximation over space (22) is used to improve the accuracy of the numerical solution. The flows through the faces of the computation cells are calculated by solving the Riemann problem. As chemical kinetics, the approximation of a laminar flame is used, with setting the chemical kinetics through the global mechanism of an oxygen-hydrogen mixture combustion (35).

Ignition of the mixture occurs on the left side of the pipe by setting the initial temperature of 1450 K in a small area (4 cells (Figure 5).

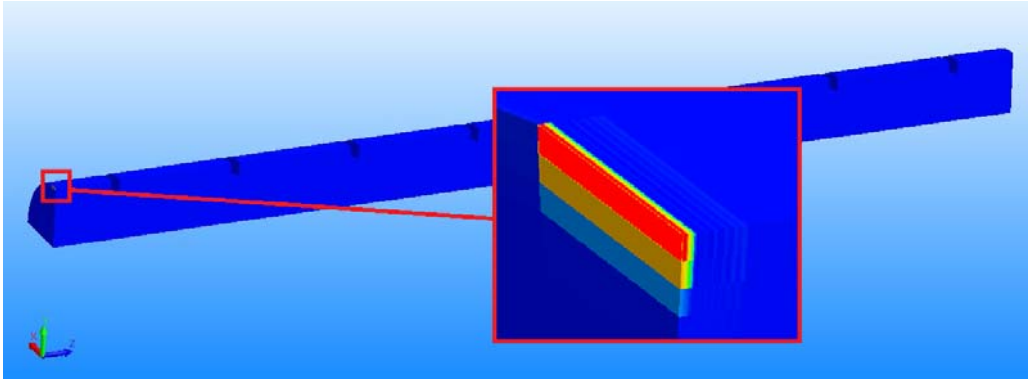

Figure 5 – Temperature field at the time point of t = 9e-06 s

Figures 6-11 further show comparative results of two computations at the time points of t = 0,0017 s and t = 0,0032 s – using one-step and multi-step hybrid schemes.

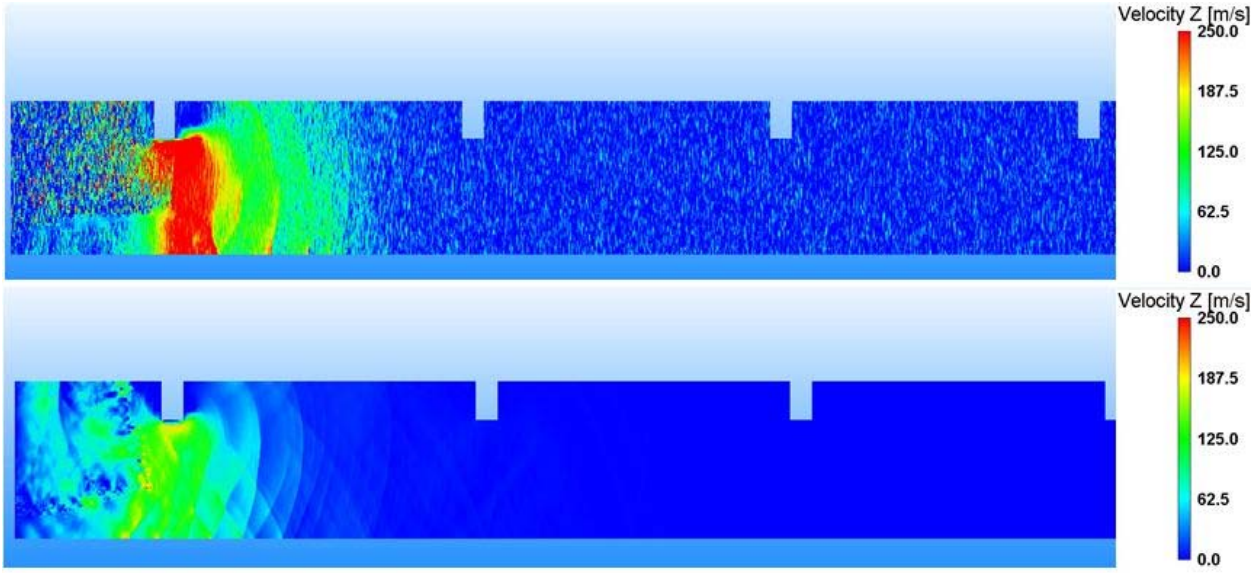

Figure 6 – Velocity profiles along axis Z at the time point t = 0,0017 s (a one-step scheme is above, a five-step scheme is below)

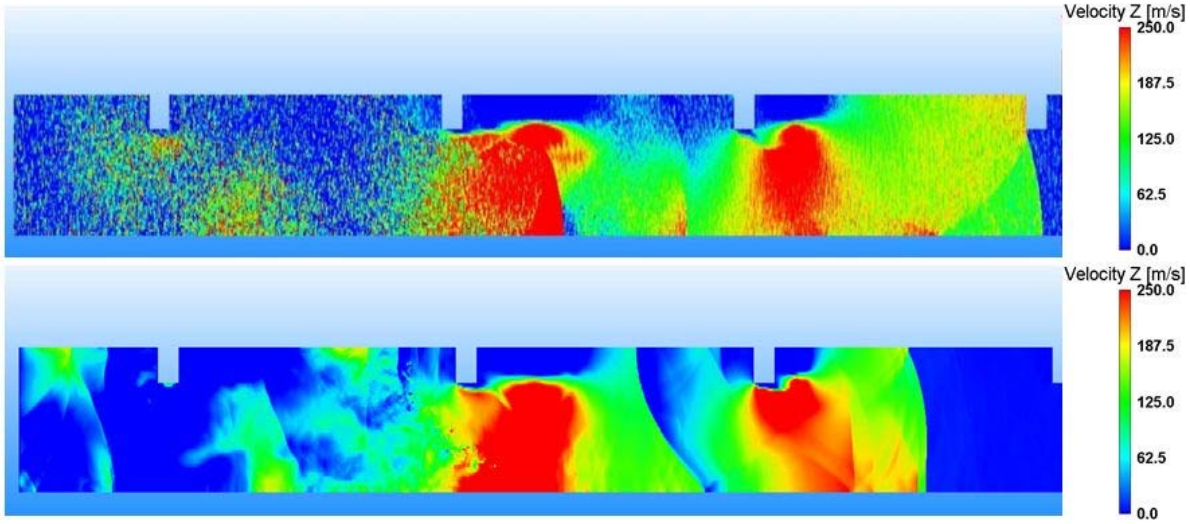

Figure 7 – Velocity profiles along axis Z at the time point t = 0,0032 s (a one-step scheme is above, a five-step scheme is below)

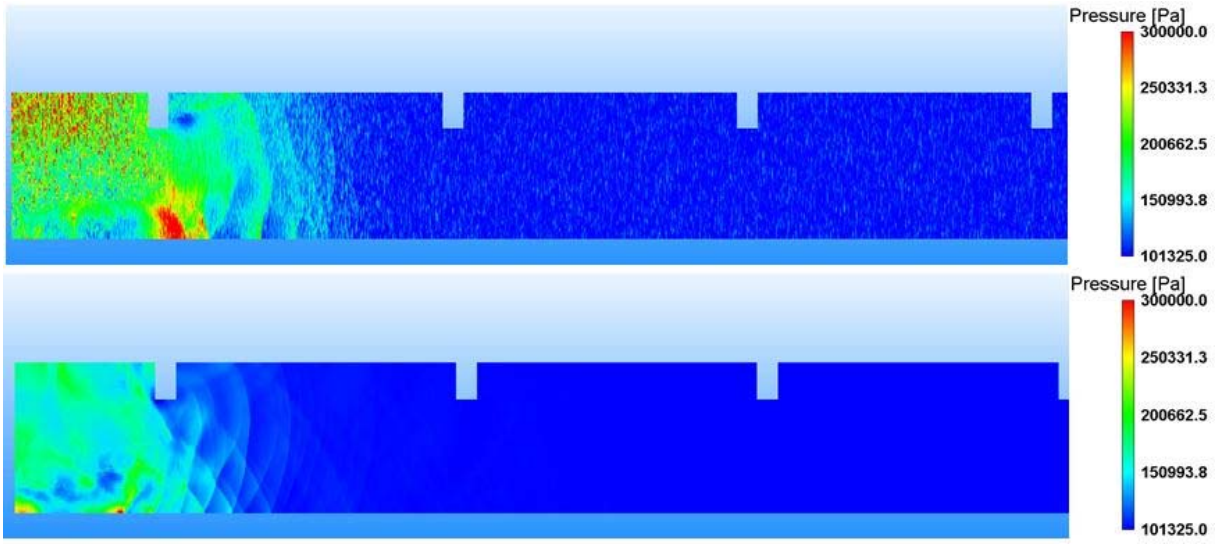

Figure 8– Pressure profiles at the time point t = 0,0017 s
(a one-step scheme is above, a five-step scheme is below)

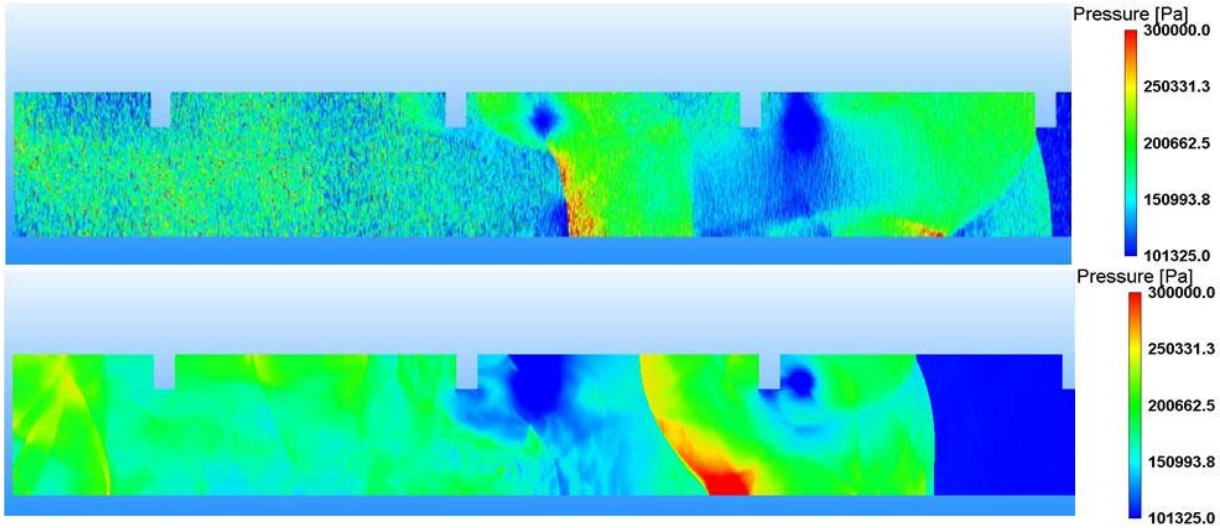

Figure 9 – Pressure profiles at the time point t = 0,0032 s
(a one-step scheme is above, a five-step scheme is below)

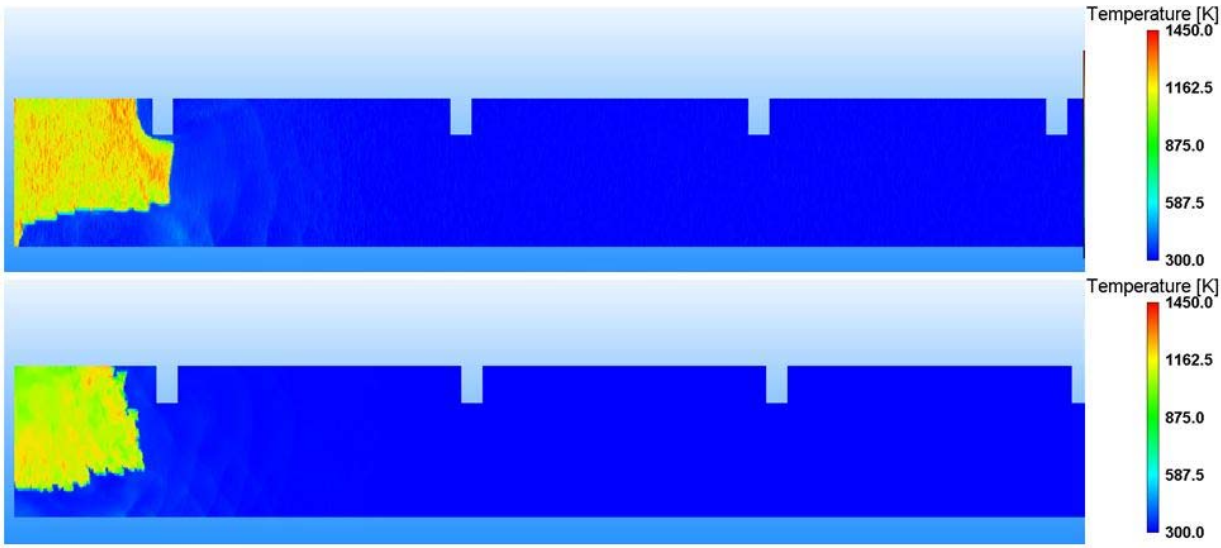

Figure 10 – Temperature profiles at the time point t = 0,0017 s
(a one-step scheme is above, a five-step scheme is below)

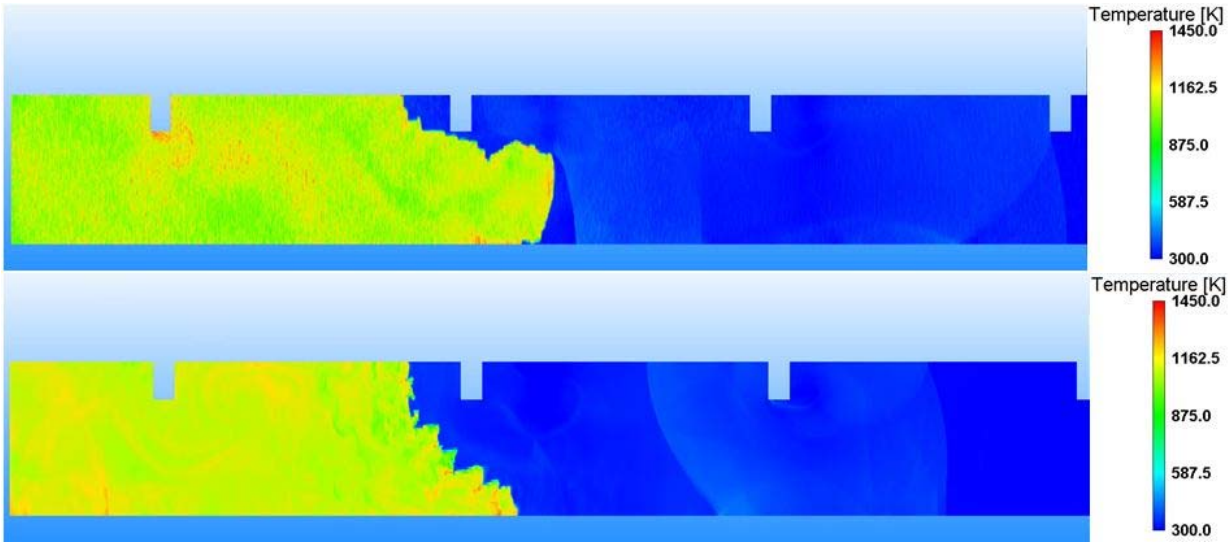

Figure 11 – Temperature profiles at the time point t = 0,0032 s
(a one-step scheme is above, a five-step scheme is below)

From the fields provided, you can see that in the solution obtained according to the one-step scheme, there are numerical oscillations that are absent when using the hybrid scheme. So, the solution obtained in the second case has greater accuracy and allows you to get a physically correct picture of the flow.

These are typical pressure distribution fields for different combustion modes - detonation and transition.

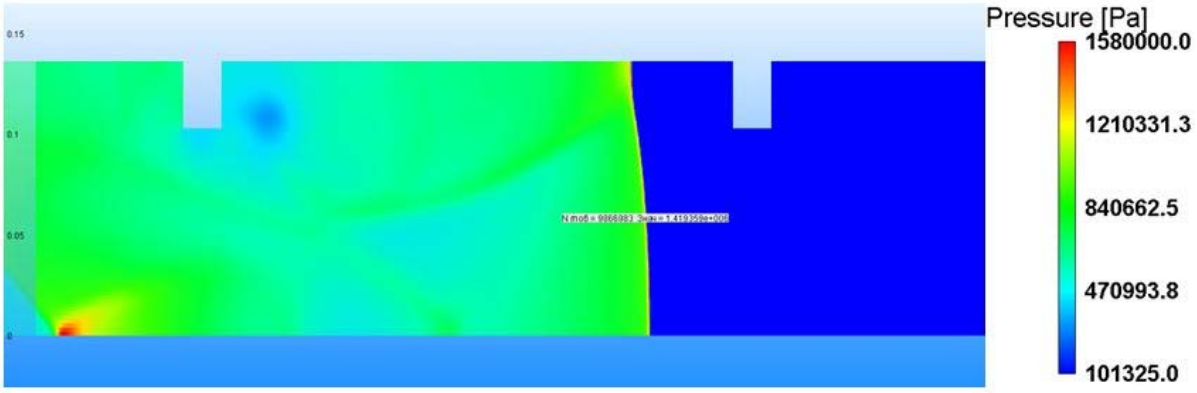

Figure 12 – Detonation combustion behavior (molar fraction of hydrogen is 16%)

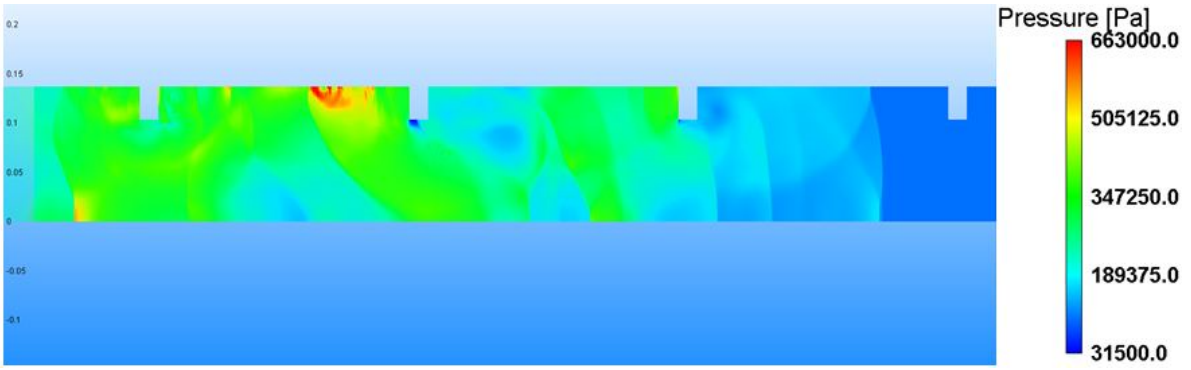

Figure 13 – Transition combustion behavior (molar fraction of hydrogen is 13%)

Table 1 shows the summary of typical front pressures and shockwave velocities derived from the hybrid scheme.

Table 1. Computation results compared to the experiment [27]

		Experiment		Computation	
# of experiment	**H2, molar percentage**	**Pressure, atm**	**Velocity, m/s**	**Pressure, atm**	**Velocity, m/s**
k21	0.158	12	1116	~16	1400
k13	0.1497	12	1058	~16	1360
k14	0.1393	4.4	868	~16	1300
k19	0.1383	3.3	843	~10-16	1260
k15	0.1272	2.7	683	2.0-6.0	400
k16	0.1183	2.3	644	1.3-3.0	430
k18	0.11	1.6	550	1.2	370
k132	0.1	combustion	combustion	no ignition	no ignition
k135	0.0857	combustion	combustion	no ignition	no ignition
k134	0.08	no ignition	no ignition	no ignition	no ignition

Experimental data show the combustion process for modes with the hydrogen concentration of more than 8%. In the computation, the combustion of the mixture was obtained at the hydrogen concentration of more than 10%, which is two modes "late" from the results of the experiment. A further increase in the concentration of hydrogen (up to 14%) results into the implementation of a "locked" combustion mode (choking), which is considered transitional, and, as a rule, has the most unstable combustion character. The detonation mode is realized at the hydrogen concentration of more than 14% - here the computation results are confirmed by the experiment. For the detonation mode, the error in determining the pressure at the front and the velocity of the shock wave does not exceed 25%. In absolute terms, this may seem an unacceptably large value. However, within the framework of the described problem, the obtained result is of practical value, since the behavior of the air mixture has been predicted, which complies with the experimental data in the case of the most complex combustion modes, depending on the concentration of hydrogen.

Conclusion

The paper describes the approach for simulating chemical processes and discusses the combustion of a hydrogen-air mixture using a Godunov-type scheme. The described model is based on the Navier-Stokes equation system, supplemented by chemical kinetics equations. The complete system of equations is approximated by the finite volume method and solved numerically using an explicit difference scheme.

In order to reduce computational costs when modeling chemical processes, a global kinetic mechanism is used based on one reaction of hydrogen oxidation, replacing the whole stage of the real kinetic process.

Using the example of the problem of simulating the combustion of a hydrogen-air mixture, it is shown that a one-step explicit scheme results into oscillations in the numerical solution. A multi-step hybrid scheme allows you to get a solution without oscillations and form a physically correct picture of the flow. As a result, flame characteristics are obtained - the speed and the pressure for various molar concentrations of hydrogen. An important result of the use of the global kinetic mechanism was the ability to predict the value of hydrogen concentration in the air mixture, at which there is a transition from its combustion to detonation. Comparison with experimental data allows us to make a conclusion about the reliability of reproducible processes obtained using the described mathematical model.

List of References

1. Kozelkov A.S., Krutyakova O.L., Kurulin V.V., Strelets D.Yu., Shishlenin M.A., The accuracy of numerical simulation of the acoustic wave propagations in a liquid medium based on Navier-Stokes equations // Siberian Electronic Mathematical Reports, 2021. http://semr.math.nsc.ru.
2. Kozelkov A.S., Struchkov A.V., Strelets D.Yu. Two Methods to Improve the Efficiency of Supersonic Flow Simulation on Unstructured Grids // Fluids 2022, 7, 136. https://doi.org/10.3390/fluids7040136.
3. Korotkov A., Kozelkov A., Three-dimensional numerical simulations of fluid dynamics problems on grids with nonconforming interfaces // Siberian Electronic Mathematical Reports, 2022. http://semr.math.nsc.ru.
4. Godunov S.K. Differential method for numerical calculation of discontinuous solutions of hydrodynamic equations // Mathem. collection. 1957. Vol. 47. № 3. pp. 271–306.
5. Godunov S.K., Zabrodin A.V., Ivanov M.Ya., Kraiko A.N., Prokopov G.P. Numerical solution of multidimensional problems of gas dynamics. M.: Nauka, 1976. 400 p.
6. Basevich V.Ya., Frolov S.M. Global kinetic mechanisms used in modeling multi-stage self-ignition of hydrocarbons in reacting currents//Chemical Physics, 2006, Vol. 25, №6, pp. 54-62.
7. Liu Wenchao. The influence of the chemical kinetics model on the results of numerical modeling of turbulent currents with combustion. Dissertation for the degree of candidate of physical and mathematical sciences. Dolgoprudny, 2023.
8. Ranzi E., Faravelli T., Gaffuri P. et al. A Wide-Ranging Modeling Study of Iso-Octane Oxidation // Combust and Flame. 1997. V. 108. P. 24
9. Glarborg P., Bentzen L.B. Chemical effects of a high CO2 concentration in oxy-fuel combustion of methane // Energy Fuels 2007, 22, 291–296.
10. Kukshinov N.V., Batura S.N., Frantsuzov M.S. Validation of methods for calculating hydrogen combustion in a supersonic flow of model air according to Beech-Evans-Schexnider experimental data. News of higher educational institutions. Mashinostroenie, 2019, № 11, p. 36–45, doi: 10.18698/0536-1044-2019-11-36-45
11. Bezgin L.V., Kopchenov V.I., Sharipov A.S., Titova N.S., Starik A.M. Evaluation of Prediction Ability of Detailed Reaction Mechanisms in the Combustion Performance in Hydrogen / Air Supersonic Flows. Combustion Science and Technology, 2013, vol. 185, iss. 1, pp. 62–94, doi: 10.1080/00102202.2012.709562
12. Zaev I.A., Prokopovich I.V. Global mechanism of self-ignition of methane: approach and construction algorithm//Chemical physics, 2014, Vol. 33, № 8, p. 3–11.
13. Strelkova M.I., Kirillov I.A., Potapkin B.V. et al. Detailed and reduced mechanisms of jet a combustion at high temperatures // Combustion Science and Technology. 2008. V. 180, Iss. 10-11. P. 1788-1802. DOI: 10.1080/00102200802258379.
14. Curran H.J., Pitz W.J., Westbrook C.K. et al. The effects of pressure, temperature and concentration of the reactivity of alkanes: experiments and modelling in a rapid compression machine // Proc. Combust. Inst. 1998. V. 27. P. 379.
15. Yakovenko I.S., Yarkov A.V., Tyurnin A.V. et al. Assessment of the possibilities of modern kinetic mechanisms of acetylene oxidation for modeling transient combustion processes. Bulletin of MSTU named after N.E. Bauman. Ser. Natural sciences, 2022, № 5 (104), pp. 62–85. DOI: https://doi.org/10.18698/1812-3368-2022-5-62-85

16. Tereza A.M., Agafonov G.L., Betev A.S., et al. Reduction of the detailed kinetic mechanism for efficient simulation of ignition delay for mixtures of methane and acetylene with oxygen. Russ. J. Phys. Chem. B, 2020, vol. 14, no. 6, pp. 951–958. DOI: https://doi.org/10.1134/S1990793120060299
17. Lebedev A.V., Okun M.V., Baranov A.E., Deminsky M.A., Potapkin B.V. Systematic procedure for simplifying the kinetic mechanisms of chemical processes //Physicochemical kinetics in gas dynamics. – 2010. – Vol. 10, № 2. – pp. 444-464.
18. Goussis D. On the construction and use of reduced chemical kinetic mechanisms produced on the basis of given algebraic relations // Journal of Computational Physics. – 1996. – Vol. 128, No. 2. – P. 261-273.
19. Andersen J., Rasmussen C.L., Giselsson T., Glarborg P. Global Combustion Mechanisms for Use in CFD Modeling under Oxy-Fuel Conditions // Energy & Fuels 2009, 23, 1379–1389.
20. Berglund M., Fedina E., Fureby C., Tegner J., Sabelnikov V. Finite Rate Chemistry Large-Eddy Simulation of Self-Ignition in Supersonic Combustion Ramjet // AIAA Journal. – 2010. – Vol. 48, No. 3. – P. 540-550.
21. Peters N., Rogg B. Reduced kinetic mechanisms for applications in combustion systems. Springer Science & Business Media, – 1993.
22. Ju Pyo Kim, Uwe Schnell, Günter Scheffknecht. Comparison of Different Global Reaction Mechanisms for MILD Combustion of Natural Gas. Combustion Science and Technology, 180:4, 565-592, 2008.
23. Sinkova O.G., Statsenko V.P., Yanilkin Yu.V. Numerical study of the transition to the detonation of hydrogen-air mixture combustion in experiments at the HTCF facility // Proceedings of RFNC-VNIIEF, №27-1, pp. 378-391, 2022.
24. Kozelkov A., Struchkov A., Zhuchkov R., Strelets D., Analysis of computational schemes for calculating gradient of fluid dynamic quantities on various grids // Aerospace Systems, https://doi.org/10.1007/s42401-024-00323-z.
25. Struchkov A., Kozelkov A., Zhuchkov R., Volkov K., Strelets D. Implementation of Flux Limiters in Simulation of External Aerodynamic Problem on Unstructured Meshes. Fluids 2023, 8(1), 31; DOI: 10.3390/fluids8010031.
26. Menshov I.S. Generalized and variational statements of the Riemann problem with application to the development of the Godunov method//Journal of Computational Mathematics and Mathematical Physics, 2020, Vol. 60, № 4, pp. 663–675.
27. Ciccarelli G., Boccio J.L., Ginsberg T., Finfrock C., Gerlach L.: The Effect of Initial Temperature on Flame Acceleration and Deflagration-to-Detonation Transition Phenomenon. Brookhaven National Laboratory, May 1998.
28. Mavriplis, D.J.; Jamson, A.: Multigrid Solution of the Navier-Stockes Equations on Triangular Meshes. AIAA Journal, 28(1990), pp. 1415-1425.
29. Landau L.D., Lifshitz E.M. Course of theoretical physics. Fluid Mechanics. Vol 6. . – New York: PERGAMON PRESS, 1959. – 541 p.
30. Loitsyanskii L. G. Mechanics of Liquids and Gases: International Series of Monographs in Aeronautics and Astronautics: Division II: Aerodynamics. – New York: PERGAMON PRESS, 1966. – 816 p.
31. Oran E. S., Boris J. P. Numerical Simulation of reactive flow. – Cambridge: Cambridge University Press. – 2001. – 550 p.
32. Schlichting H. Boundary-Layer Theory. 7th edition – New York: Springer, 1979. – 838 p.

33. Leveque R.J. Finite-Volume Methods for Hyperbolic Problems // Cambridge University Press, 2002.
34. Kozelkov A.S., Galanov N. G., Semenov I. V., Zhuchkov R. N., Strelets D. Yu., Computational Investigation of the Water Droplet Effects on Shapes of Ice on Airfoils. Aerospace 2023, 10, 906. https://doi.org/10.3390/aerospace10100906.
35. Blazek J. Computational Fluid Dynamics: Principles and Applications. – New York: Elsevier, 2001. – 496 p.
36. Toro E.F. Riemann solvers and numerical methods for fluid dynamics, 3-rd edition. Springer-Verlag, Berlin, 2009, 724 p.
37. Van Leer B. Towards the ultimate conservative difference scheme V: A second-order sequel to Godunov's method // J. Comp. Phys. 1979. V. 32. P. 101–136.
38. Rodionov A.V. Increasing the order of approximation of the S.K. Godunov scheme // Journal of Computational Mathematics and Mathematical Physics. 1987. Vol. 27. № 12. pp. 1853–1860.
39. Harten A., Osher S. Uniformly high-order accurate non-oscillatory schemes // Int. J. of Numerical Analys. 1987. V. 24. № 2. P. 279–310.
40. Jameson A., Schmidt W., Turkel E. Numerical Solutions of the Euler Equations by Finite Volume Methods Using Runge-Kuttn Time-Stepping Schemes. AIAA Paper 81-1259, 1981.
41. Marinov N.M., Westbrook C. K., Pitz W.J. Detailed and Global Chemical Kinetics Model for Hydrogen // Lawrence Livermore National Laboratory // P.O. Box 808, L -298, Livermore, CA. 94551, USA, 1995.